



## Preparation and Characterization of Prism-Like ZnO with Pore Structure†

H.M. HU<sup>1,\*</sup>, C.H. DENG<sup>2</sup>, Q. FANG<sup>1</sup>, K.H. ZHANG<sup>1</sup>, M. SUN<sup>1</sup> and H. XUAN<sup>1</sup>

<sup>1</sup>School of Materials and Chemical Engineering, Anhui University of Architecture, Hefei, P.R. China

<sup>2</sup>Department of Chemical and Materials Engineering, Hefei University, Hefei, P.R. China

\*Corresponding author: Tel: +86 551 3828100; E-mail: hmhu@ustc.edu

AJC-11286

Porous zinc oxide microprisms constructed by connected nanoparticles have been successfully prepared by thermal decomposition of the Zn-N<sub>2</sub>H<sub>4</sub> complexes precursor at 600 °C for 1 h in air, which was synthesized in advance using Zn(CH<sub>3</sub>COO)<sub>2</sub>·2H<sub>2</sub>O as zinc source and hydrazine hydrate as complexing agent through a room-temperature coordination-precipitation technique. The morphology of ZnO inherit that of the precursor. The products were characterized by X-ray diffraction, energy dispersive X-ray spectrometry, field-emission scanning electron microscopy, UV-visible absorption spectrum and photoluminescence spectrum.

**Key Words:** ZnO, Pore structure, Thermal decomposition, Nanomaterials.

### INTRODUCTION

Recently, porous materials have attracted many interest because they have broad applications in many fields, ranging from bioengineering, catalysis, separation and environmental engineering to chemical and gas sensors, due to their large specific surface area, high porosity and increased mass transport in the porous materials<sup>1-3</sup>. Zinc oxide, a remarkable *n*-type semiconductor oxide with a direct wide band gap of 3.37 eV, non-linear optical property and large exciton binding energy of 60 meV at room temperature, has aroused considerable attention due to potential applications in solar cells, optoelectronic devices, gas sensors, photocatalysts, optical waveguides, surface acoustic wave transducers, *etc.*<sup>4,9</sup>.

Various methods have been attempted to synthesize ZnO with porous architectures. Zou *et al.*<sup>10</sup> prepared porous ZnO ribbons by oxidation of ZnS ribbons at an annealing temperature of 700 °C in the air. Yacaman *et al.*<sup>11</sup> synthesized porous single crystalline ZnO nanodisks with sponge-like morphology through a wet chemical approach. Li *et al.*<sup>12</sup> fabricated porous ZnO nanotubes with 250 nm diameter, 40 nm wall thickness and 500 nm length *via* a facile hydrothermal method. Jiang *et al.*<sup>13</sup> synthesized porous octahedron- and rod-shaped ZnO architectures by thermal decomposition of ZnC<sub>2</sub>O<sub>4</sub>·2H<sub>2</sub>O precursors. Wu *et al.*<sup>14</sup> prepared hierarchical porous ZnO disc-like nanostructures for photovoltaic applications through a simple low-temperature hydrothermal method. Zhang *et al.*<sup>15</sup>

fabricated monodisperse porous ZnO sheres by a facile and low-cost soluble-starch-assisted method. Huang *et al.*<sup>16</sup> synthesized porous ZnO flower-like nanostructures by a template-free hydrothermal method combined with subsequent calcination. Huang *et al.*<sup>17</sup> prepared porous ZnO nanosheets growing on copper substrates by a chemical bath deposition technique followed by a heat treatment.

In this paper, a convenient environmental friendly two-step method was developed to prepare porous ZnO prism. The Zn-N<sub>2</sub>H<sub>4</sub> complex precursor was firstly synthesized by a room-temperature coordination-precipitation route. The pre-obtained precursors was then thermal-decomposed at 600 °C for 1 h in air to form prism-like ZnO with abundant pore structure.

### EXPERIMENTAL

All chemicals (analytical grade reagents) were purchased from Shanghai Chemical Reagents Co. and used without further purification.

#### General procedure:

**Preparation of precursors:** In a typical procedure, 12.75 g zinc acetate dihydrate (Zn(CH<sub>3</sub>COO)<sub>2</sub>·2H<sub>2</sub>O) was dissolved in 100 mL deionized water in a 200 mL beaker. 20 mL hydrazine hydrate (N<sub>2</sub>H<sub>4</sub>·H<sub>2</sub>O 85 %) was subsequently added into the above solution under stirring. White suspension with small solid was rapidly produced. After stirring for 20 min, the beaker was placed in a refrigerator (5 °C) ageing for 20 h. The resulting white precursors were filtered off, washed with distilled water

†Presented to The 5th Korea-China International Conference on Multi-Functional Materials and Application.

for several times and then finally dried in a vacuum at 60 °C for 4 h. The collected precursors were signed as sample A.

**Preparation of porous ZnO:** 0.5 g precursors was put into a 60 mL crucible and then transferred into a resistance furnace and heated to 600 °C in air with a ramping rate of 5°C/min, then calcined at 600 °C for 1 h under ambient pressure. The collected calcined products were signed as sample B.

**Detection method:** The phase purity of the as-synthesized products was examined by X-ray diffraction (XRD) using a Dandong Y-2000 X-ray diffractometer equipped with graphite monochromatized  $\text{CuK}\alpha$  radiation ( $\lambda = 1.54178 \text{ \AA}$ ). Field-emission scanning electron microscope (FESEM) images of the samples were taken on a field-emission microscope (Sirion 200, 15kV) attached with the energy dispersive X-ray spectrometry (EDX). UV-visible spectrum was studied using a UV-vis spectrophotometer (UV-2550). Photoluminescence (PL) spectrum was recorded on a Laser MicroRaman Spectrometer (JYLABRAM-HR) using the 325 nm exciton of the He-Cd laser at room temperature.

## RESULTS AND DISCUSSION

Fig. 1(a) shows XRD patterns of precursor (sample A) and calcined product (sample B). From the XRD pattern of sample A, it was observed that the precursor prepared at room temperature has good crystallinity. Because these diffraction peaks can not be accurately indexed, it was presumed that the precursor is a coordination compound (named as  $\text{Zn-N}_2\text{H}_4$  complexes) produced by the complexing reaction of  $\text{Zn}(\text{CH}_3\text{COO})_2 \cdot 2\text{H}_2\text{O}$  and  $\text{N}_2\text{H}_4 \cdot \text{H}_2\text{O}$ . From the XRD pattern of sample B, all the diffraction peaks can be indexed to wurtzite structure of ZnO with lattice parameters  $a = 3.248 \text{ \AA}$  and  $c = 5.203 \text{ \AA}$ , in good agreement with the reported data for ZnO (JCPDS File, 5-664,  $a = 3.249 \text{ \AA}$ ,  $c = 5.205 \text{ \AA}$ ). No characteristic peaks belonging to other impurities were detected. The sharp diffraction peaks indicate the good crystallinity of the as-prepared ZnO products. The purity and composition of the as-prepared sample are also reflected by EDX analysis (Fig. 1(b)). The result exhibits only the presence of Zn and O elements in products. The molar ratio of Zn:O obtained from the peak areas is 0.96:1.00, which is in agreement with stoichiometry of ZnO. A peak assigned to aluminium are due to background from aluminum foil.

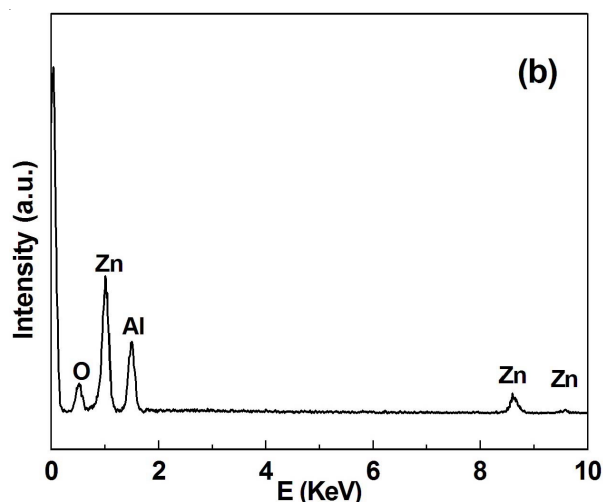
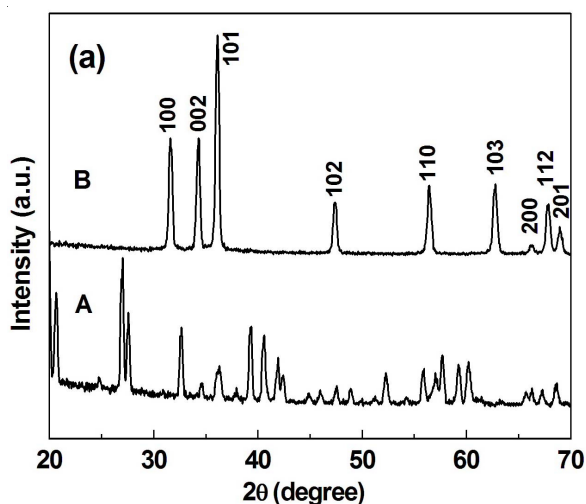
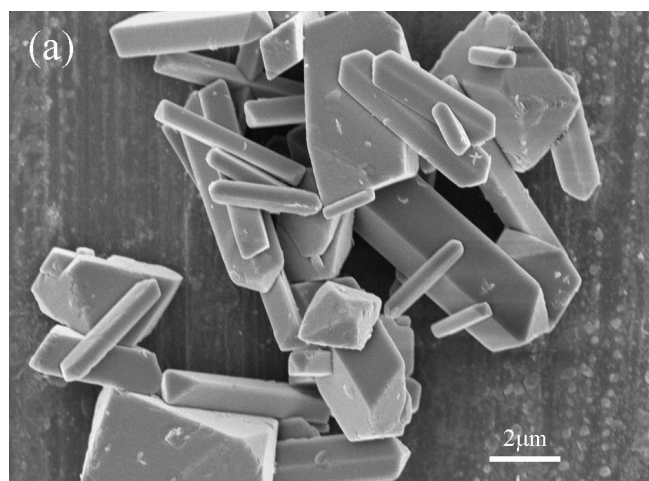


Fig. 1. (a) XRD patterns of precursors and calcined products, (b) EDX spectrum of calcined products

The morphologies of precursors and ZnO products were detected by FESEM. The as-prepared precursor and ZnO take on similar morphologies are shown in Figs. 2. Fig. 2(a) and 2(b) give the pictures of precursor obtained through a room-temperature coordination-precipitation technique using  $\text{Zn}(\text{CH}_3\text{COO})_2 \cdot 2\text{H}_2\text{O}$  and hydrazine hydrate as starting raw material. Based on the observation of FESEM images, prism-like microstructures as well as a small number of polyhedrons are found in the preobtained precursor. The diameter of prism ranges from 0.5  $\mu\text{m}$  to 4.0  $\mu\text{m}$  and the length is about 3-5  $\mu\text{m}$ . The surfaces of these precursors micropisms are quiet smooth. Fig. 2(c) and (d) show the morphologies of ZnO products obtained by calcinating precursors at 600 °C for 1 h in air, which indicates that the ZnO products basically retain the morphologies of precursors. The ZnO products mainly exhibit prim-like morphologies coexisting with a little polyhedrons, which are composed of 80-120 nm nanoparticles arranged irregularly in original direction of precursors. By contrast, the surfaces of ZnO micropisms are considerably rough. The pore structure was clearly observed in Fig. 2(d). The pore diameter was estimated to be 50-300 nm.

During the process of heat treatment, we find that the morphology and pore structure of ZnO crystals were greatly affected by calcinated temperature. To evaluate the effect of



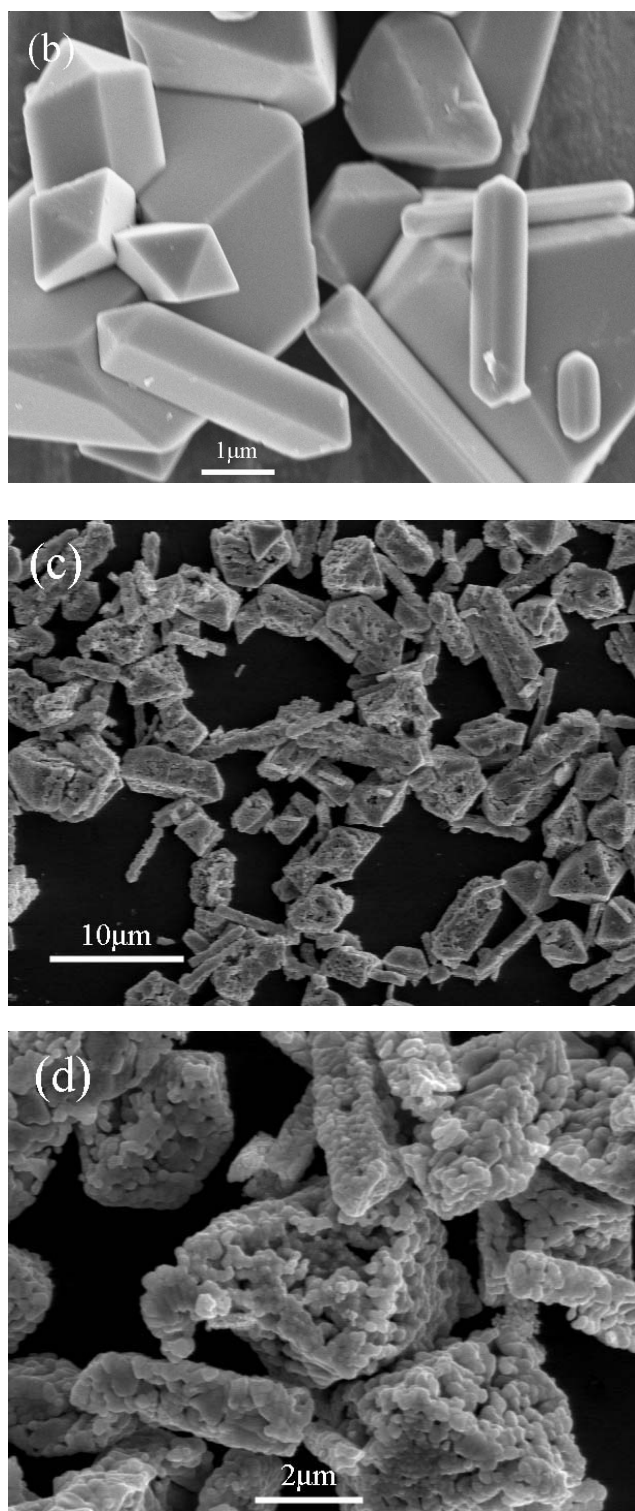


Fig. 2. (a,b) FESEM images of precursors, (c,d) FESEM images of ZnO products obtained by calcinating precursors at 600 °C for 1h

calcinated temperature, we carried out two comparative experiments by only changing calcinated temperature and simultaneously keeping other conditions unchanged. Fig. 3(a) is the FESEM image of ZnO obtained by calcinating precursors at 400 °C for 1 h in air, which shows that fissures appear on the surfaces of ZnO crystals. A lot of holes are found on the surfaces of ZnO crystals when the calcinated temperature was increased to 500 °C [Fig. 3(b)].

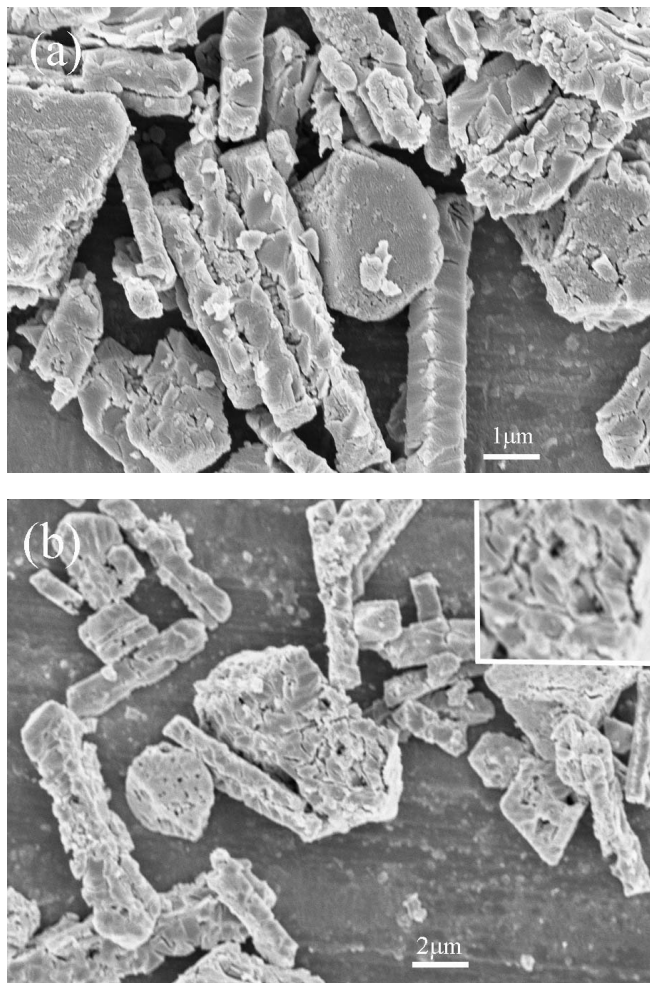


Fig. 3. FESEM images of ZnO products obtained by calcinating precursors at different temperature: (a) 400 °C, (b) 500 °C

Fig. 4(a) shows UV-vis absorption spectrum of the as-synthesized porous ZnO microprisms dispersed in deionized water at room temperature. A strong and sharp peak located at 375 nm in ultraviolet region was clearly observed, which is similar to the bulk absorption of ZnO<sup>18</sup>. Fig. 4(b) presents the room-temperature photoluminescence spectrum of the porous ZnO microprisms. An intense, sharp and dominated peak at 387 nm in the UV region and a suppressed and broad green emission band at 514 nm in the visible region are observed. The UV peak of ZnO is related to the excitation emission<sup>19</sup>. The green-light emission of ZnO corresponded to the singly ionized oxygen vacancies and its recombination with a photo-generated hole<sup>20</sup>.

### Conclusion

In conclusion, by employing a convenient two-step method, ZnO microprisms with abundant pore structures have been successfully synthesized. UV-vis absorption spectrum of the porous ZnO microprisms shows that the peak position is similar to the bulk absorption of ZnO. The room temperature photoluminescence spectrum of the porous ZnO microprisms shows a good optical property in UV region. The present method is convenient, environmental friendly and without using any organic additive, which may be used to controllably synthesize other porous metal oxide with particular morphology.

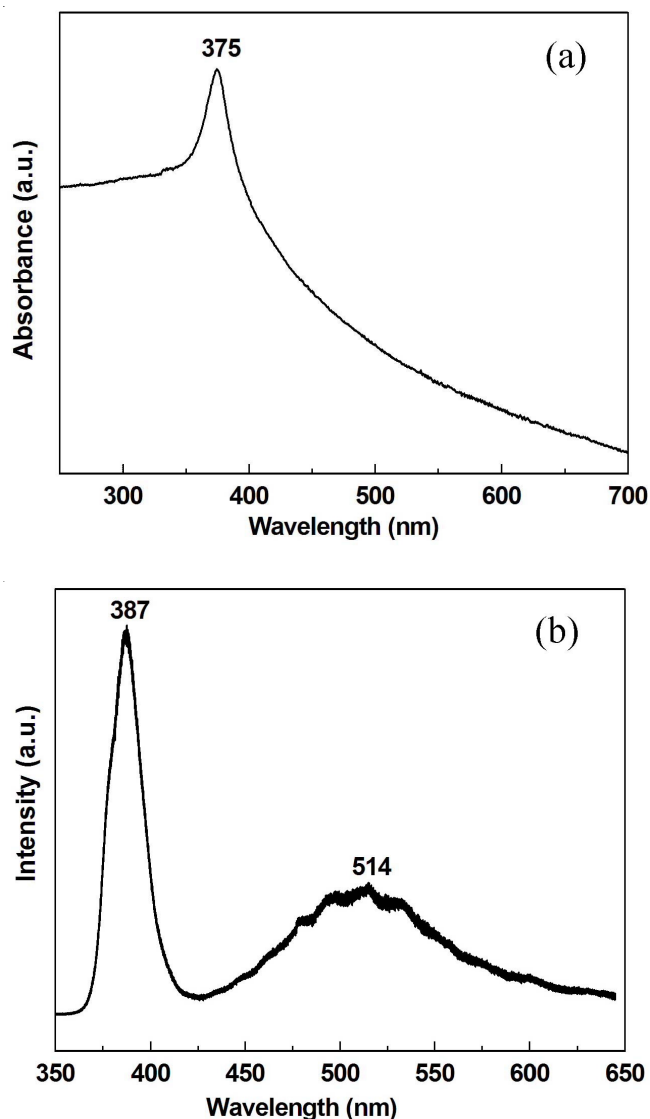


Fig. 4. UV-vis absorption spectrum (a) and PL spectrum (b) of the porous ZnO microprisms

## ACKNOWLEDGEMENTS

This work was supported by the Fifth Science and Technology Foundation of Outstanding Youth of Anhui Province (Grant No. 10040606Y25), the Science and Research Foundation for Development of Hefei University (Grant No. 11KY01ZD) and the National Natural Science Foundation of China (Grant No. 20501002).

## REFERENCES

1. L. Tosheva and V.P. Valtchev, *Chem. Mater.*, **17**, 2494 (2005).
2. I.I. Slowing, B.G. Trewyn, S. Giri and V.S. Lin, *Adv. Funct. Mater.*, **17**, 1225 (2007).
3. J.Y. Liu, T. Luo, F.L. Meng, K. Qian, Y.T. Wan and J.H. Liu, *J. Phys. Chem. C*, **114**, 4887 (2010).
4. K. Keis, E. Magnusson, H. Lindstrom, S.E. Lindquist and A. Hagfeldt, *Sol. Energy*, **73**, 51 (2002).
5. S. Cho, J. Ma, Y. Kim, Y. Sun, K.L. Wong and J.B. Ketterson, *Appl. Phys. Lett.*, **75**, 2761 (1999).
6. J. Zhang, S.R. Wang, M.J. Xu, Y. Wang, B.L. Zhu, S.M. Zhang, W.P. Huang and S.H. Wu, *Cryst. Growth Des.*, **9**, 3532 (2009).
7. N. Kaneva, I. Stambolova, V. Blaskov, Y. Dimitriev, S. Vassilev and C. Dushkin, *J. Alloys Compd.*, **500**, 252 (2010).
8. F.C.M. Van De Pol, *Ceram. Bull.*, **69**, 1959 (1990).
9. M. Kadota, *Jpn. J. Appl. Phys. Part 1*, **36**, 3076 (1997).
10. F.F. Wang, R.B. Liu, A.L. Pan, S.S. Xie and B.S. Zou, *Mater. Lett.*, **61**, 4459 (2007).
11. B. Reeja-Jayan, E. De la Rosa, S. Sepulveda-Guzman, R.A. Rodriguez and M.J. Yacamán, *J. Phys. Chem. C*, **112**, 240 (2008).
12. H.Q. Wang, G.H. Li, L.C. Jia, G.Z. Wang and C.J. Tang, *J. Phys. Chem. C*, **112**, 11738 (2008).
13. J. Zheng, Z.Y. Jiang, Q. Kuang, Z.X. Xie, R.B. Huang and L.S. Zheng, *J. Solid State Chem.*, **182**, 115 (2009).
14. J.X. Wang, C.M.L. Wu, W.S. Cheung, L.B. Luo, Z.B. He, G.D. Yuan, W.J. Zhang, C.S. Lee and S.T. Lee, *J. Phys. Chem. C*, **114**, 13157 (2010).
15. G.K. Zhang, X. Shen and Y.Q. Yang, *J. Phys. Chem. C*, **115**, 7145 (2011).
16. C.P. Gu, J.R. Huang, Y.J. Wu, M.H. Zhai, Y.F. Sun and J.H. Liu, *J. Alloys Compd.*, **509**, 4499 (2011).
17. X.H. Huang, X.H. Xia, Y.F. Yuan and F. Zhou, *Electrochim. Acta*, **56**, 4960 (2011).
18. A.B. Djuricic and Y.H. Leung, *Small*, **2**, 944 (2006).
19. B.D. Yao, Y.F. Chan and N. Wang, *Appl. Phys. Lett.*, **81**, 757 (2002).
20. K. Vanheusden, W.L. Warren, C.H. Seager, D.K. Tallant, J.A. Voigt and B.E. Gnade, *J. Appl. Phys.*, **79**, 7983 (1996).